Linear Programming for Real-Time Renewable Energy Operation in Low Energy Buildings

Hamza El Hafdaoui
School of Science and Engineering
Al Akhawayn University in Ifrane
Ifrane, Morocco
h.elhafdaoui@aui.ma

Ahmed Khallaayoun
School of Science and Engineering
Al Akhawayn University in Ifrane
Ifrane, Morocco
a.khallaayoun@aui.ma

***Abstract* — This study presents a model for day-ahead load and renewable energy scheduling, utilizing Support Vector Regression to enhance 24-hour electricity prediction. The optimization of scheduling incorporates linear programming for real-time renewable energy operations, exploring the scenarios of photovoltaic without storage, photovoltaic with storage and no-feed-in-tariff, and photovoltaic with storage and feed-in-tariff in low energy buildings. The envisioned real-time efficient renewable energy operation involves the adoption of microgrids for electricity export and energy management. Through experimental validation on a residential building in Ifrane, Morocco, the forecasting model demonstrates an average error rate of ±8.71%. Notably, with a 4 kWp rated photovoltaic power system, the building operates autonomously during the day, acting as a positive energy structure by exporting surplus energy to the grid. In the photovoltaic with a battery and no-feed-in-tariff scenario, the building aims for energy autonomy, pursuing a zero-energy building status while exporting excess energy. In the feed-in-tariff scenario, the algorithm manages electricity storage and export, but post-midnight, grid electricity remains necessary, categorizing the residential building as a low-energy structure. Finally, while the model has broad applicability, the findings of the case study are limited.**

Keywords — Linear programming, policy based algorithm, integration optimization, building energy management, energy management system, microgrid, renewable energy, low energy building.

I. Introduction

A. Overview and Background

The global energy landscape is significantly impacted by buildings, which account for more than one-third of total energy consumption and the consequent greenhouse gas emissions [1, 2]. Concurrently, the operational aspects of buildings hold substantial promise for achieving energy conservation and carbon mitigation [2, 3]. In the pursuit of decarbonization, the building sector emerges as a pivotal player, with a focus on energy efficiency, substituting fossil fuel end-use with electricity, and incorporating a significant share of renewable energy resources for power generation [4-6]. As efforts to curtail carbon emissions intensify, advancements in the electrification and renewable energy integration in the building sector present increasingly pronounced challenges to the functioning of the current power grid [3, 7, 8].

As buildings undergo changes in electricity consumption due to electrification, the integration of renewable energy introduces heightened variability and irregular power generation patterns. This dynamic often leads to challenges such as power outages and curtailment, arising from the misalignment between energy supply and demand [9]. A potential solution to mitigate these issues involves the creation of microgrids, which integrate buildings and other energy systems. The strategic operation of these microgrids has the potential to alleviate pressure on the main grid, offering a promising avenue for addressing the aforementioned challenges [10].

B. Low Energy Buildings

Microgrids serve as a vital link connecting energy consumers, such as buildings, to distributed energy generation and storage systems. The integration of photovoltaic (PV) systems and batteries plays a significant role in the pursuit of decarbonization and electrification [11]. While most microgrids may not operate entirely independently, effective management of energy systems presents an opportunity to minimize dependence on and disturbances from the main grid when required.

The significance of microgrids is paramount in the context of zero energy buildings and nearly zero energy buildings, with the latter being a specialized subset of the former. While the principles underlying both concepts are well-established, there exists no universally standardized definition for either. However, there is a widespread consensus that a (nearly) zero energy building is characterized by its energy efficiency, wherein the primary energy consumption is effectively offset by the renewable energy generated within the building itself. In essence, these buildings aim to achieve a balance between energy demand and renewable energy production, marking a pivotal step towards sustainability and reduced environmental impact. In the subsequent sections of the paper, the term "nearly zero energy building" will be referred to as "low-energy building." This unified terminology aims to streamline the discussion and enhance clarity regarding the various energy-efficient building concepts under consideration.

C. Literature Review

The definitions provided have spurred numerous researchers worldwide to delve into various studies concerning the concept of low-energy buildings and the optimization of renewable energy systems within. Despite this, a noticeable gap remains in the literature regarding real-time renewable energy operation in (nearly) zero and low zero energy buildings [12-15].

Balakumar et al. [12] introduced a demand-side management program within a smart grid framework to mitigate the peak-to-average ratio of utility grids and reduce end-users' electricity tariffs. The incorporation of renewable energy, coupled with an energy storage system in the demand-side management controller, aims to enhance both economic and environmental aspects for end-users. This article puts forward a novel approach using a Recurrent Neural Network (RNN)-based Long Short-Term Memory (LSTM) framework for minute-by-minute and 5-minute intervals forecasting of electric power consumption and renewable energy generation specifically for the Science Block (SCB). The performance of

National Center for Scientific and Technical Research in Morocco (CNRST)

this proposed deep learning model is assessed through metrics such as mean squared error, mean absolute error, root mean square error, and R-squared. The results demonstrate the effectiveness of the proposed demand-side management program in providing tangible benefits to end electricity users and contributing positively to the operations of smart grid operators.

Rawa et al. [13] introduced a seasonal optimization framework for short-term microgrid operation, incorporating energy storage and solar PV systems. The model considers day-ahead microgrid scheduling, addressing the influence of varying climatic factors on resource optimization throughout the year. The study employs the converged barnacles mating optimizer to solve the resulting single-objective optimization problem effectively. Simulation results indicate a reduction in the total operating cost of the grid-integrated microgrid.

Mukhopadhyay and Das [14] employed the grey wolf optimizer within a fuzzy formulation for the long-term optimal sizing of renewable-based distributed generators and battery energy storage systems. The objectives for sizing optimization include minimizing total annual expenses, yearly emissions, and yearly energy loss, while maximizing the annualized monetary benefit from deferring network upgrades. The integration of distributed energy resources is strategically designed to defer network upgrades, resulting in significant financial benefits for the utility. An optimal hourly power schedule is obtained for the microgrid, incorporating a selective price-based demand response strategy to accommodate seasonal variations in renewable power generation and demand. The profitability of the microgrid prosumer is enhanced through the demand response program, which promotes increased utilization of renewable power. The study implements hourly probabilistic modeling to address uncertainties in renewable power and consumer demand.

Rashid et al. [15] introduced an enhanced energy and cost minimization approach for residential consumers aimed at shaping peak loads and utility tariffs. The study presents a power management algorithm utilizing renewable energy sources and energy storage systems, implemented through C++ language. The effectiveness of the proposed power management algorithm techniques is assessed across three distinct scenarios, with extensive case studies validating their benefits. The results indicate significant energy and cost savings of up to 34% and 45%, respectively, compared to existing methods, underscoring the efficacy of the proposed energy and cost minimization scheme.

D. Novelty, Objectives, and Outline

The methodologies outlined in the literature review seek to minimize energy costs by fully leveraging renewable energy systems within buildings. Nevertheless, a discernible gap exists in the adaptability of these algorithms to low-energy buildings, where considerations extend beyond mere energy optimization and cost reduction to include environmental impact.

The model considers day-ahead load and renewable energy scheduling, addressing the influence of varying climatic factors on resource optimization throughout the year. The primary goal of this study is to decrease grid energy consumption in a building equipped with a renewable energy system (PV) and a storage system (battery), thereby reducing grid dependence and environmental impact. To achieve the objectives, a linear programming algorithm determines the timing and quantity of energy storage or release from the battery, optimizing electrical energy exchange with the grid. The objective function is designed to penalize high grid energy usage, aligning with the principles of low-energy buildings. Additionally, forecasted data on load demand and PV generation contribute to global optimization throughout the day. Real energy requirement data from a residential building in Ifrane, Morocco, is utilized to showcase the effectiveness of the optimization algorithm in practical applications.

The paper is organized into four sections. In the Methodology (Section II), a comprehensive overview of the architecture, forecasting model, and optimization model is provided. The Results and Analysis (Section III) explores three optimization-case scenarios utilizing the linear programming algorithm. The optimization and analysis focus on load balance, battery storage levels, and optimum dispatch for scenarios without storage, with storage and no feed-in-tariff, and with storage and feed-in-tariff for a case study of a residential building in Ifrane, Morocco. Lastly, the Conclusion

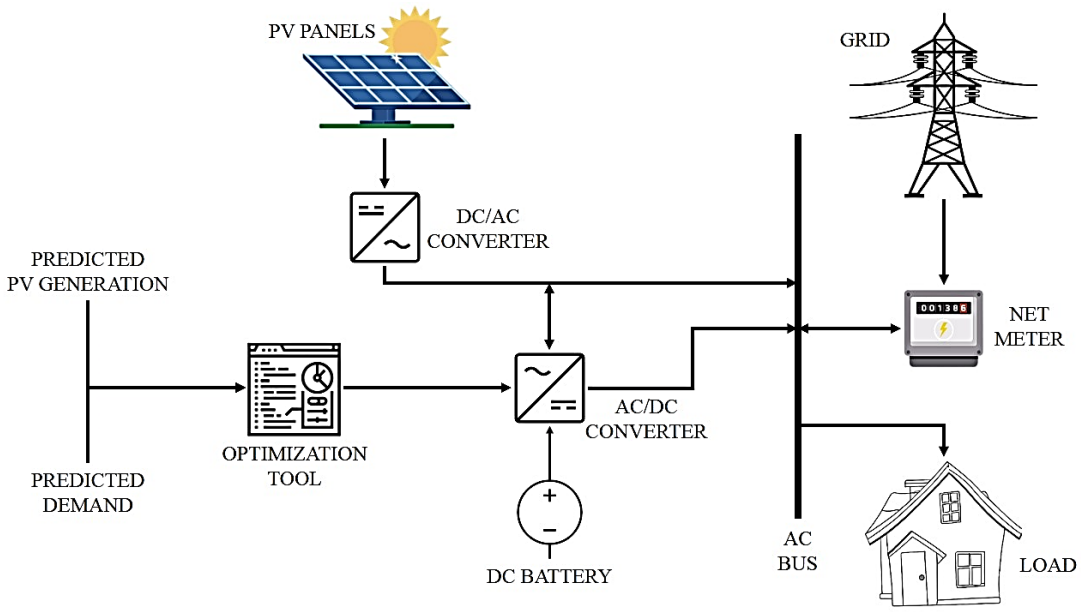

Fig. 1. Diagram of System Architecture

(Section IV) summarizes the work, discusses the study's limitations, and outlines potential avenues for future research.

II. Methodology

A. Architecture

This section provides a brief overview of the system architecture outlined in the paper. The optimization algorithm is fed forecasted data for the upcoming 24 hours, encompassing PV generation and load demand. The forecasted data are generated based on Support Vector Regression (SVR).

The optimization model is focused on efficiently managing the charging/discharging of the battery system. This is achieved through linear programming based on the forecasted data. The primary goal is to maximize PV utilization while optimizing the energy exchange with the grid, considering the applicable tariff scheme. The algorithm runs daily at midnight, ensuring global optimization by utilizing forecasted data for the upcoming 24 hours. Figure 1 presents a simplified diagram of the proposed system, highlighting the incorporation of net metering technology.

B. Forecasting Model

The forecasting model is Support Vector Regression (SVR), adopted from Zhang et al. [16]. Support Vector Regression is a regression algorithm derived from Support Vector Machines (SVM), designed to predict continuous values. In the context of 24-hour electricity prediction for a building, SVR employs a kernel trick to transform the input space, facilitating the identification of a hyperplane that minimizes the error between predicted and actual values. The algorithm incorporates a loss function with a regularization term to manage model complexity and avoid over fitting. Notably, SVR introduces the concept of an epsilon-insensitive tube, allowing a margin of tolerance for prediction errors. Hyperparameters, such as c (cost of error) and ε (error boundary), play a crucial role in tuning the model's performance, balancing the trade-off between fitting the training data and generalizing to new data [17]. By training SVR on historical data, including time of day and weather conditions, it becomes a valuable tool for forecasting electricity consumption over the next 24 hours, aiding in efficient renewable energy utilization for the building.

In situations where datasets are not linearly separable, requiring mapping to an N-dimensional space for an (*N-1*)-dimensional separating hyperplane, the computational complexity can be high. The kernel trick comes into play as a practical solution, substantially reducing computational costs. The relationship between input variables $x_1, x_2, \ldots, x_3$ and the output Y is established through a kernel function $\varphi(x)$ in (1), introducing coefficients W and b. These coefficients are determined by minimizing (2) subject to defined constraints in (3) and (4), where w represents a weight vector, and c denotes the cost associated with prediction errors. The constraints involve residuals beyond the boundary ϵ, depicted as ε_i and ε_i^*, emphasizing the trade-off between fitting the data and controlling for errors in the context of Support Vector Regression.

$$Y = W.\varphi(x) + b \tag{1}$$

Objective:

$$\frac{1}{2}\|w\|^2 + c.\frac{1}{N}.\sum_{i=1}^{N} \varepsilon_i + \varepsilon_i^*\Big|_{min} \tag{2}$$

Constraints:

$$y_i + w^T.\varphi(x_i) - b \leq \epsilon + \varepsilon_i \tag{3}$$

$$w^T.\varphi(x_i) + b - y_i \leq \epsilon + \varepsilon_i^* \tag{4}$$

The investigation encompasses both hourly and daily granularities, with a focus on assessing the accuracy of predictions. Figure 2 provides a visual representation of the framework employed for individual building electrical forecasting, outlining key stages such as data processing, exploratory data analysis, prediction, and evaluation. The unprocessed dataset obtained from smart meters includes electricity consumption data measured in kilowatt-hours (kWh) for buildings, recorded on an hourly time scale. Additionally, historical hourly weather and humidity data are sourced from Meteonorm (v8.0). Finally, the Mean Absolute

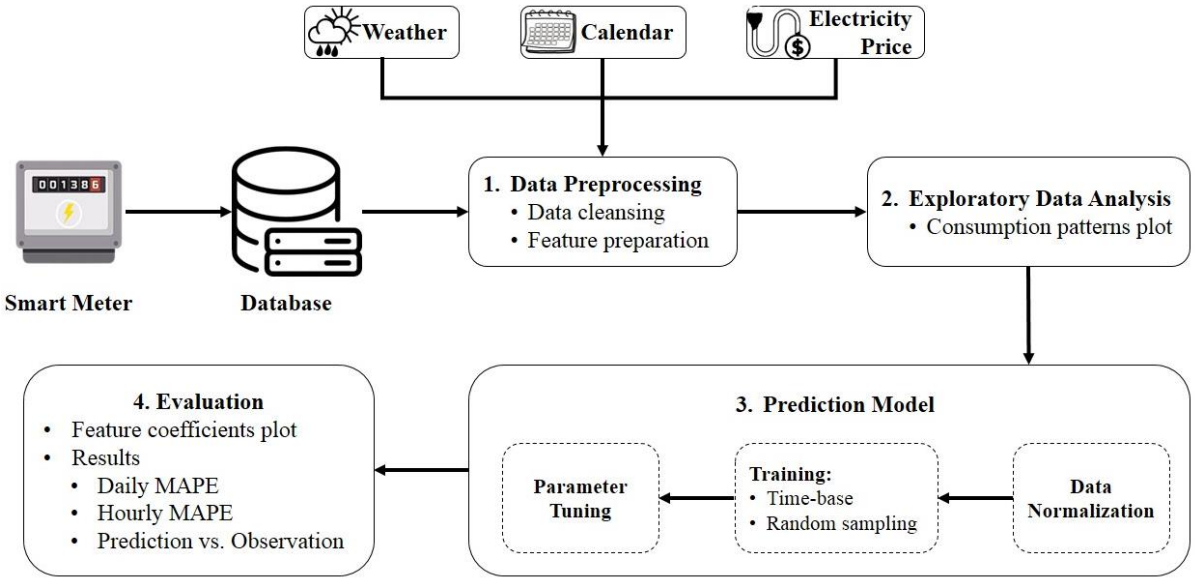

Fig. 2. Framework of Individual Building Electricity Forecasting

Percentage of Error (MAPE) is used in the evaluation phase to measure the prediction accuracy of the model. The MAPE equation, depicted in (5), involves actual electricity consumption y_j, predicted consumption $\widehat{y_j}$, and the total number of observations n.

$$MAPE\ (\%) = \frac{100}{n}\sum_{j=1}^{n}\left|\frac{y_j - \widehat{y_j}}{y_j}\right| \quad (5)$$

C. Optimization Model

In the realm of optimization, a non-linear problem assumes convexity when both its objective functions exhibit convex behavior and its constraints follow an affine pattern. The distinctive advantage of engaging in convex optimization lies in the availability of robust and efficient algorithms capable of yielding a global optimal solution, provided it exists. This advantageous outcome becomes particularly attainable when a non-linear problem, whether convex or not, can be adeptly transformed into a linear problem, falling under the category of convex problems.

The formulation of the initial non-linear (convex) problem is encapsulated in Equations (6)–(14). Herein, P_{grid} symbolizes the net grid power, representing the disparity between the powers imported/exported from/to the grid in kilowatts (kW) — adopting a negative value for exported power and a positive one for imported power. The variable k signifies the hour of the day, C_{grid} denotes the electricity cost in USD per kilowatt-hour ($/kWh), and Δt stands for the time step in hours, set to 1 in this scenario, corresponding to an hourly basis. Further variables include PV for the PV power generated in kilowatts (kW), P_{bat} representing the charging/discharging rate of the battery (negative for discharging and positive for charging), $LOAD$ indicating the instantaneous demand in kilowatts (kW), SOC representing the storage level of the battery in kilowatt-hours (kWh), P_{bat}^{max} indicating the maximum discharge/charging rate of the battery in kilowatts (kW), PV^{max} representing the power rating of the PVs in kilowatts (kW), $LOAD^{max}$ indicating the maximum allowable demand in kilowatts (kW), and SOC^{min} as well as SOC^{max} representing the minimum and maximum capacity of the battery, respectively, in kilowatt-hours (kWh).

Objective:

$$P_{grid}\big|_{min} = \sum_{k}^{24}\left(C_{grid}(k).\left|P_{grid}(k)\right|.\Delta t\right) \quad (6)$$

Constraints:

$$LOAD(k) = PV(k) - P_{bat}(k) + P_{grid}(k) \quad (7)$$

$$SOC(k) = (P_{bat}(k) \times \Delta k) + SOC(k-1) \quad (8)$$

$$\begin{cases} \Delta k = 1 \\ SOC(0) = c \end{cases} \quad (9)$$

$$P_{grid}(k) \le LOAD(k) \quad (10)$$

$$-P_{bat}(k) \le LOAD(k) \quad (11)$$

$$-P_{bat}^{max} \le P_{bat}(k) \le P_{bat}^{max} \quad (12)$$

$$-PV^{max} \le P_{grid}(k) \le LOAD^{max} \quad (13)$$

$$SOC^{min} \le SOC(k) \le SOC^{max} \quad (14)$$

The focal point of our optimization lies in (6), the objective function that demands minimization, while the ensuing expressions, (7)–(14), delineate the tangible constraints and demarcations intrinsic to our predicament. A prospect of easing the complexity of our conundrum beckons by excising (10) and (11), responsible for precluding both the direct charge of the battery from the grid and the direct export of energy from the battery to the grid. Nonetheless, the removal of these constraints may usher in voltage and frequency imbalances within the grid, potentially giving rise to battery-related quandaries attributable to the unpredictable surge in battery operations throughout the day.

Within the realm of low-energy buildings, the aspiration is to minimize the energy imported from the grid, ideally driving it as close to zero as feasible. This pursuit is encapsulated by the absolute term in (1), where the overarching goal is to curtail the net grid power. The elimination of the absolute term, under ideal circumstances, propels the optimization towards the objective function approaching negative infinity, signifying an unbounded lower limit. Consequently, in this scenario, all the energy generated by PV systems and stored in batteries would be directed towards export to the grid. The algorithm specifically seeks to minimize grid dependency, making this configuration less desirable in the context of energy-efficient structures.

In an ideal scenario, the optimal resolution for the aforementioned problem is achieved when the grid power, denoted as $P_{grid}(k)$, equals zero. However, in practical implementation, factors such as varying generation patterns, demand fluctuations, and initial storage levels may prevent the net grid energy from reaching absolute zero. Instead, the optimization aims to achieve the optimal minimization of this net grid energy, taking into account the dynamic interplay of generation, demand, and storage conditions.

The non-linearity inherent in (6) owing to the presence of the absolute term prompts the exploration of linearization techniques. One effective approach involves expressing the variable $P_{grid}(k)$ as the difference between two non-negative slack variables [18, 19], as in (15) for the condition in (16). Furthermore, the term $C_{grid}(k)$ can be expanded linearly, capitalizing on its inherent linearity. This transformation allows us to demonstrate that the initial non-linear problem encapsulated in (1) can be equivalently represented as a linear problem, subject to the condition that $C_{grid}(k)$ remains non-negative for all instances of *k*. The resulting linear formulation is articulated in (17), providing a tractable and linearized representation of the original non-linear problem. In the expression, $C_{grid}^{export}(k)$ and $C_{grid}^{import}(k)$ denote the selling price and cost of electricity to/from the grid, respectively, measured in $/kWh. On the other hand, $P_{grid}^{export}(k)$ signifies the surplus PV power directed towards the grid, while on the other hand $P_{grid}^{import}(k)$ represents the grid power imported into the system.

$$P_{grid} = P_{grid}^{export}(k) - P_{grid}^{import}(k) \quad (15)$$

$$\forall k \in [0,24]; \{P_{grid}^{export}(k), P_{grid}^{import}(k)\} \ge 0 \quad (16)$$

$$(C_{grid}^{export}, C_{grid}^{import}, P_{grid}^{export}, P_{grid}^{import}\big|_{min} = \sum_{k=1}^{24}\left(C_{grid}^{export}(k).P_{grid}^{export}(k).\Delta t + C_{grid}^{import}(k).P_{grid}^{import}(k).\Delta t\right) \quad (17)$$

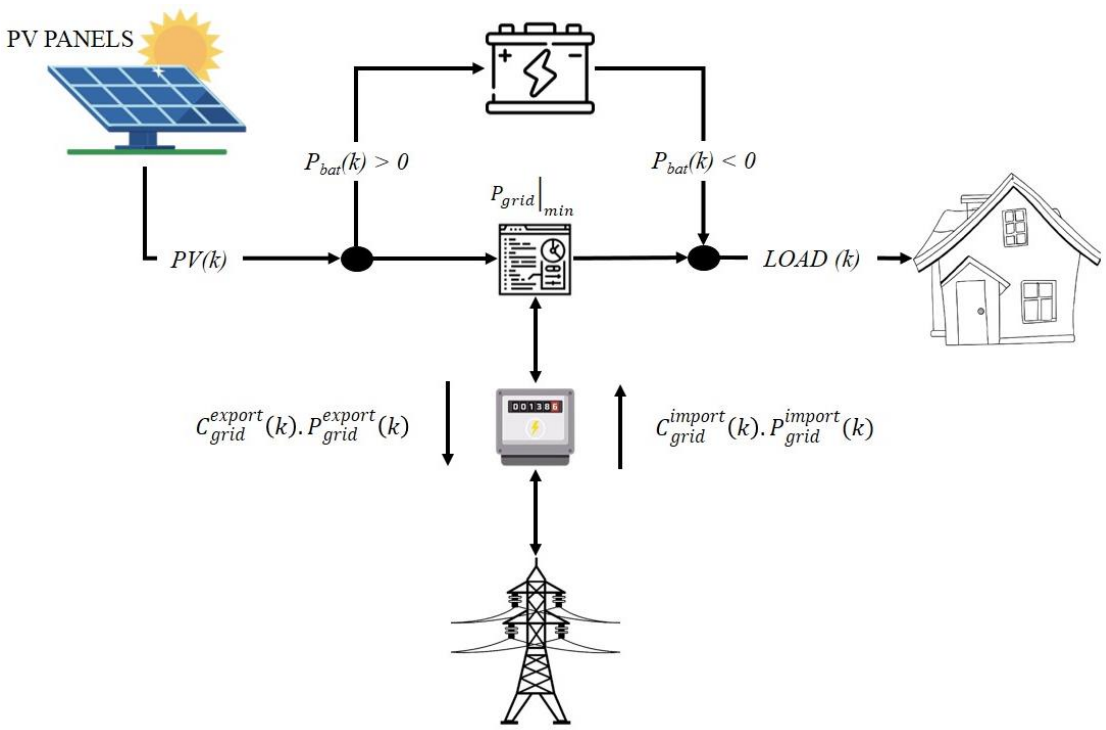

Fig. 3. Graphical Illustration of the Optimization Model

Equations (6) and (17) may not be identical, but they are equivalent, sharing the same optimized solution. It is important to emphasize that the product of the two slack variables consistently equals 0 throughout the optimization process. For example, if, for any reason, the optimal value of the objective function exceeds 0 – a common scenario in real-world problems – it logically follows that the subsequent optimal value of the objective must be either $P_{grid}^{export}(k)$ or $P_{grid}^{import}(k)$. This inference arises from the fact that both variables are invariably greater than 0. This observation underscores a crucial property; at optimality, the condition stipulated in (18) is consistently satisfied. This property is pivotal, as it obviates the need for additional constraints to address the condition in (16), which may not hold in practical situations.

$$P_{grid}^{export}(k) \times P_{grid}^{import}(k) = 0 \tag{18}$$

In residential sectors of certain countries where there is no feed-in-tariff for selling PV energy to the grid, matrix $C_{grid}^{export}(k)$b turns positive. In such cases, it can be assigned a small value, as illustrated in (19). Maintaining a positive value for $C_{grid}^{export}(k)$ is essential, as it plays a crucial role in the objective function. Omitting this term from the objective function would result in $P_{grid}^{export}(k)$ consistently assuming the highest possible values. This outcome is undesirable in scenarios lacking a feed-in-tariff scheme.

$$C_{grid}^{export}; \begin{cases} C_{grid}^{export} \to 0 \\ C_{grid}^{export}(k) \neq 0, \forall k \in [0,24] \end{cases} \tag{19}$$

Figure 3 visually conveys the linear problem, providing a graphical depiction of the flow of various powers and delineating the node associated with the objective function. It is important to note that this representation specifically reflects the scenario where the battery is restricted from drawing or supplying power to the grid. To address and solve the optimization problem, *linprog()* function in MATLAB is employed. This function serves as a computational tool for linear programming, facilitating the efficient resolution of the linearized problem.

III. Results and Analysis

In the context of a residential building located in Ifrane, characterized by insulation, a southeast orientation, and specific U-values for walls (0.50 W/m².K), roofs (0.42 W/m².K), and glazing (1.95 W/m².K), an 5 kW-rated battery with a storage capacity of 10 kWh is deployed alongside a 4 kW-rated PV system. Notably, the overall U-value of this residential structure aligns with the thermal construction regulations outlined in Morocco [18].

It is noteworthy that the cost of electricity acquisition is contingent upon the prevailing rates set by the national electricity contractor, ONEE. A detailed breakdown of electricity prices for residential buildings based on consumption levels is provided in Table 1. The case study assumes a microgrid implementation in Ifrane.

Table 1. Prices of electricity for residential buildings in Ifrane

Electricity Consumption per Month	Price ($/kWh)
0 to 100 kWh	0.09
101 to 200 kWh	0.11
201 to 300 kWh	0.12
301 to 500 kWh	0.14
> 500 kWh	0.16

Empirical data for both PV generation and load demand on a fall, usual workday (October 12th, 2023) in Ifrane, Morocco, have been accurately predicted. Given the U-value of the residential building, no heating is required on the allocated day. The load data specifically mirrors the demand

profile of a residential building accommodating four residents, characterized by low energy consumption.

Figure 4 illustrates the forecasted load and PV generation. The forecast was generated 11:59 pm on October 12th, 2023 and includes the prediction of load and PV generation for the following day up to 11:59 pm of October 13th, 2023. Upon experimental validation, the percent of error was averaged in ±8.71%. As the figure shows, the load of the building is significantly lower than the PV profile from 8 am to 6 pm. During that time period of the day, electricity is stored in the battery or exported to the microgrid.

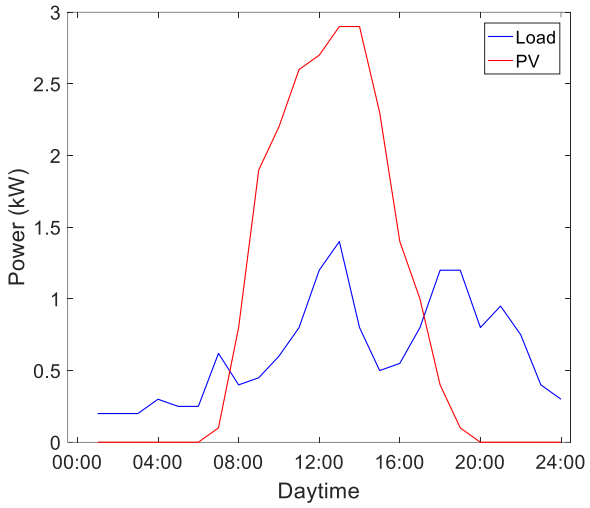

Fig. 4. Load and PV Profiles Forecast

Morocco lacks a feed-in-tariff program for Net-Metering customers if their yearly energy output surpasses their annual grid consumption. Consequently, the end-user's advantage diminishes further. The suggested model factors in both purchasing electricity from and selling it to the grid. Specifically, if a feed-in-tariff exists—where customers are compensated for exporting solar energy—matrix $C_{grid}^{export}(k)$ becomes negative and receives corresponding value assignments. The optimization scenarios include the operation without storage, the operation with storage – no feed-in-tariff, and the operation with storage – feed-in-tariff.

A. *Operation without Storage*

Initially, a scenario depicts an existing PV installation without a battery. In this scenario, PV energy is exported to the grid, and the user is charged based on the net energy consumed. The term$C_{grid}^{import}(k)$ is determined according to the monthly electricity consumption outlined in Table 1. In Figure 5, the optimized power balance is presented for a low-energy building with a PV system, operating without a battery, and functioning under a non-feed-in-tariff scheme. A considerable amount of the PV energy is observed to be exported to the grid due to the reduced load. The daily electricity cost in this scenario amounts to $0.62.

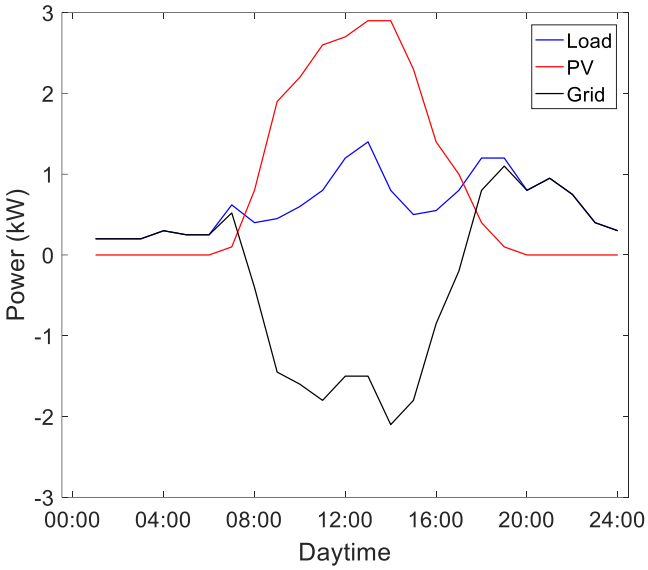

Fig. 5. Load Balance Operation without Storage

B. *Operation with Storage – No-Feed-in-Tariff*

In the absence of a feed-in-tariff, the values of $C_{grid}^{import}(k)$ and $C_{grid}^{export}(k)$ coincide. Various scenarios, each with distinct initial storage levels represented by *SOC(0)*, have been explored to analyze the fluctuations in net grid power and electricity costs. Figure 6 illustrates the load balance in the presence of energy storage without a feed-in-tariff (FIT) assuming a null initial state of charge, and results reveal the role of battery storage in reducing $P_{grid}^{import}(k)$ in the residential building thus reduced environmental impacts.

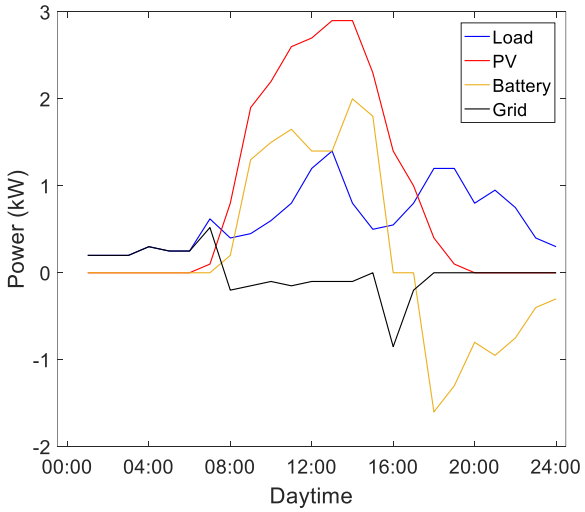

Fig. 6. Load Balance Operation with Storage and No-FIT

According to Figure 6, the battery initially had no stored energy as assumed. The load, on the other hand, is positive, indicating the need for electricity in the residential building. However, the required power is minimal at 1 am. Between 7 and 8 am, the PV system begins generating electricity, reaching its peak around 2 pm. In the morning, the load demand is lower compared to the PV generation, allowing the battery to be charged during that time. Simultaneously, a small amount of electricity is exported to maintain a balanced state of charge in the battery. Between 3 and 5 pm, the battery becomes fully charged (Figure 7), while the PV system generates more electricity than the load requires. Consequently, all excess electricity is exported to the

microgrid. Starting at 5 pm, the load exceeds the PV generation, leading to the utilization of stored electricity in the battery. By midnight, the remaining state of charge in the battery is 3.9 kWh, indicating that the initial energy stored the following day equals *SOC(24)*. In this scenario, there is a high probability that electricity import will be negligible the next day.

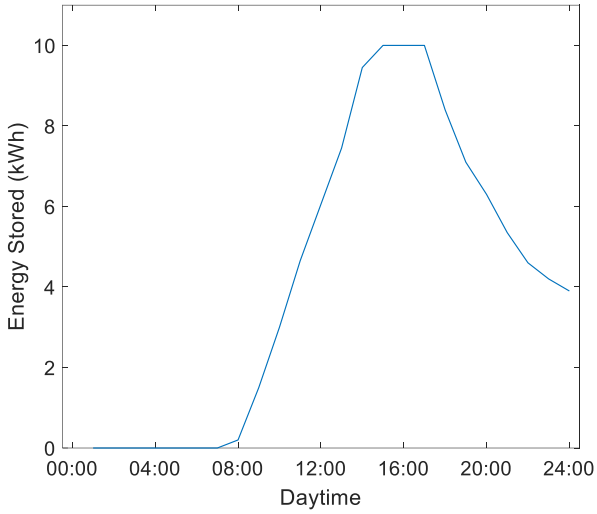

Fig. 7. Electricity Stored in Battery with No-FIT

In the provided operational scenario with *SOC(0)*, Figure 8 illustrates the optimal dispatch. The residential building relies on grid electricity imports from midnight to 7 am. From 7 am to 6 pm, the building exclusively depends on PV generation. Concurrently, any surplus electricity generated during this period is stored in the battery and exported to the grid. Between 7 am and midnight, the electricity source shifts to the battery, ensuring a continuous power supply for the building.

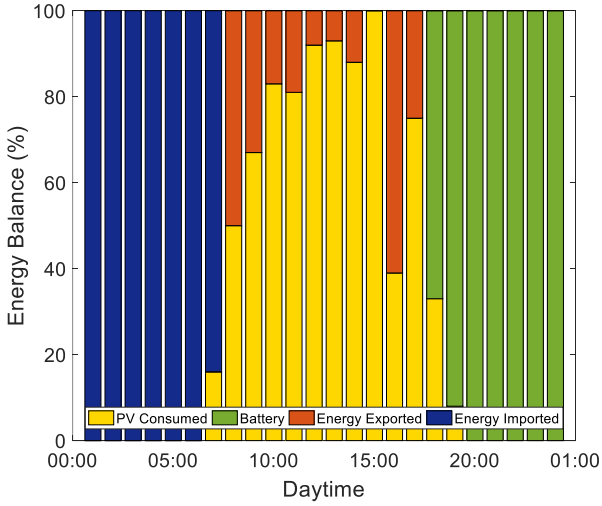

Fig. 8. Optimum Dispatch with No-FIT

As emphasized earlier, the outcomes presented in Figures 6-8 are significantly influenced by the initial state of charge of the battery. Consequently, parameters such as P_{grid}, C_{grid}^{import}, C_{grid}^{export} are subject to variation based on the initial storage conditions. This variability in the initial state of charge has a direct impact on load balance, energy storage, and the optimal dispatch strategy throughout the day. Therefore, it is crucial to consider the initial SOC as a key factor in analyzing and interpreting the observed changes in grid power, import and export costs, and overall system behavior.

C. Operation with Storage – Feed-in-Tariff

In the last scenario under consideration, the end-user benefits from receiving compensation for excess PV energy in a feed-in-tariff scheme, where the export cost $C_{grid}^{export}(k)$ exceeds the import cost $C_{grid}^{import}(k)$ for all time steps k. To gain insights into the optimization behavior, it is assumed that the selling price exceeds 10% of the purchase price. Additionally, the initial state of charge of the battery is assumed to be null. This implies that the battery starts with no stored energy, and the system aims to maximize the economic gains by prioritizing the sale of surplus PV energy to the grid when energy imports are not foreseen during the same day.

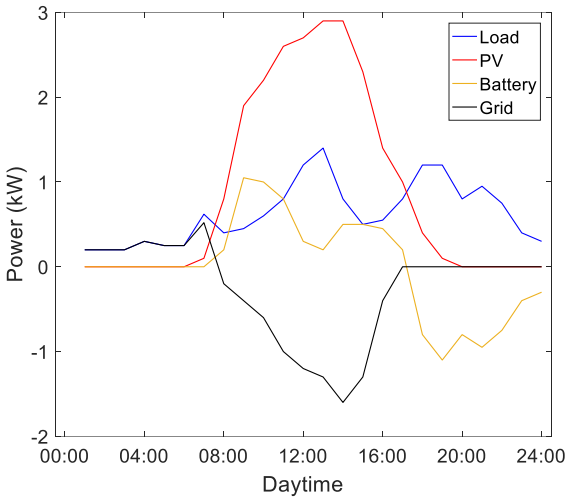

Fig. 9. Load Balance Operation with Storage and FIT

Comparing the output in Figure 6 with the results in Figure 9, $P_{grid}^{export}(k)$ has significantly increased under the feed-in-tariff scheme. However, the algorithm still prompts to store electricity in the battery to suffice the electricity needs in the day given the forecasted load. Figure 10 shows the electricity stored in the battery under the feed-in-tariff scheme, as previously stated, the state of charge becomes null by the end of the day.

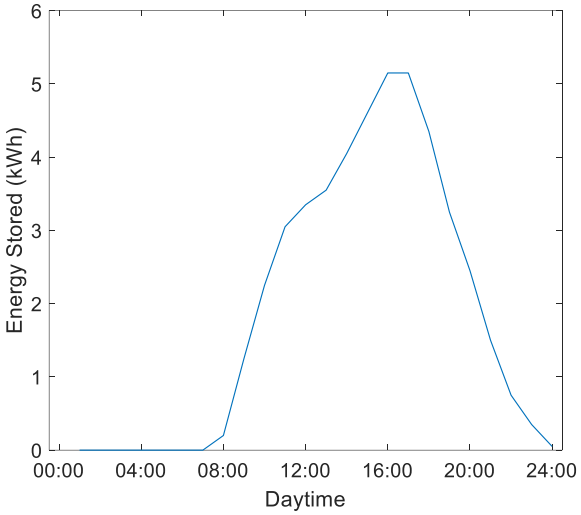

Fig. 10. Electricity Stored in Battery with FIT

As depicted in Figure 11, the algorithm exhibits distinct behavior under a feed-in-tariff framework. If the initial state

of charge is considered, the outcomes would have omitted the electricity imported from the grid. Nevertheless, the study assumed a zero electricity charge for k=0. Additionally, the algorithm under the feed-in-tariff scheme could be adjusted to prioritize storing adequate electricity until 7 am of the next day, rendering it suitable for zero-energy buildings.

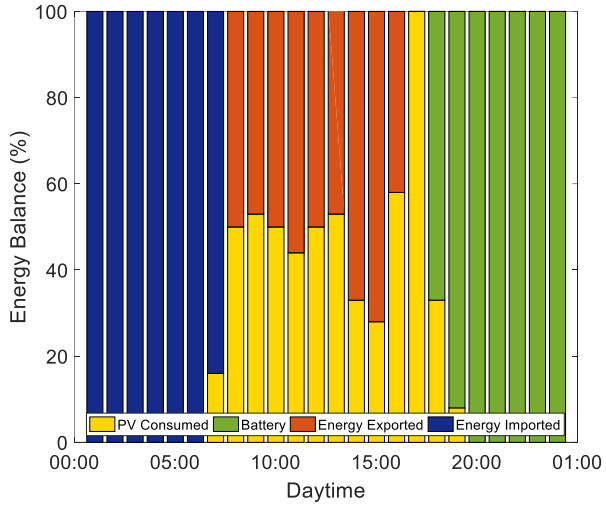

Fig. 11. Optimum Dispatch with FIT

IV. Conclusion

In conclusion, this study presents a model for day-ahead load and renewable energy scheduling. The forecasting model, Support Vector Regression (SVR), utilizes a kernel trick to transform input space for 24-hour electricity prediction. Derived from Support Vector Machines, SVR predicts continuous values by identifying a hyperplane minimizing the error between predicted and actual values. For scheduling optimization, linear programming was adopted for real-time renewable energy operation of PV without storage, PV with storage and no-feed-in-tariff, and PV with storage and feed-in-tariff in low energy buildings. The real-time efficient renewable energy operation in the model assumes the adoption of microgrids or smart grids for electricity export and energy management.

In analyzing a residential building in Ifrane, Morocco, the forecasting model exhibited an average error rate of ±8.71% following experimental validation. The building features a 4 kWp rated PV power system. In scenarios without storage, the building relies on grid electricity at night but operates independently during the day through autonomous PV electricity generation. Surplus energy is exported to the grid, categorizing it as a positive energy building; however, significant environmental impact arises from nighttime grid electricity imports. In the PV with battery and no-feed-in-tariff scenario, assuming a 5 kW-rated battery with a 10 kWh capacity, the building prioritizes energy autonomy. It generates and stores electricity in the battery, aiming for a zero-energy building. Excess renewable energy is exported to the grid as denoted by $C_{grid}^{export}(k)$ when stored energy is abundant. In the PV with battery and feed-in-tariff scenario, the algorithm balances electricity storage and export, storing enough for daily needs until midnight. Nevertheless, grid electricity is still required post-midnight, classifying the residential building as a low-energy building.

While the model possesses a broad applicability, it is crucial to acknowledge that the conclusions drawn from the case study are confined to specific parameters. These parameters include the load profile of the building, the rated power of the renewable energy system, the assumed initial state of charge, and the horizontal solar irradiance characteristic of Ifrane. To enhance the robustness and comprehensiveness of the findings, future studies should deliberately challenge the algorithm by exploring various load profiles, testing multiple rated powers for the renewable energy system, examining a range of initial state of charge conditions from null to maximum, and considering different levels of horizontal solar irradiance. Expanding the scope of the investigations to encompass diverse scenarios and conditions will not only validate the model's versatility but also provide insights into its adaptability across a broader spectrum of real-world situations. This approach will contribute to a more nuanced understanding of the algorithm's performance under varied circumstances, thereby ensuring its reliability and efficacy across a diverse range of applications. Consequently, the generalizability of the model can be further validated, making it a more robust tool for addressing the complexities and the variability inherent in renewable energy systems and building energy management.

Acknowledgment

This work was supported by the National Center for Scientific and Technical Research in Morocco (CNRST) within the framework of '***Development of Smart Metering and Energy Management System in Morocco***'.

References

[1] Global Alliance for Buildings and Construction, "Global Status Report for Buildings and Construction," United Nations Environment Programme (UNEP), 2020.

[2] International Energy Agency (IEA), "World Energy Outlook," Paris, France, 2023.

[3] H. El Hafdaoui, A. Khallaayoun and K. Ouazzani, "Long-term low carbon strategy of Morocco: A review of future scenarios and energy measures," *Results in Engineering*, vol. 21, p. 101724, 2024.

[4] H. El Hafdaoui, A. Khallaayoun and K. Ouazzani, "Activity and Efficiency of the Building Sector in Morocco: A Review of Status and Measures in Ifrane," *AIMS Energy*, vol. 11, no. 3, pp. 454-485, 2023.

[5] H. El Hafdaoui, A. Khaldoun, A. Khallaayoun, A. Jamil and K. Ouazzani, "Performance Investigation of Dual-Source Heat Pumps in Hot Steppe Climates," in *3rd International Conference on Innovative Research in Applied Science, Engineering and Technology (IRASET*, Mohammedia, Morocco, 2023.

[6] O. Bamisile, C. Dongsheng, J. Li, H. Adun, R. Olukoya, Bamisile¸Oluwatoyosi and Q. Huang, "Renewable energy and electricity incapacitation in sub-Sahara Africa: Analysis of a 100% renewable electrification in Chad," *Energy Reports*, vol. 9, no. Supplement 10, pp. 1-12, 2023.

[7] H. El Hafdaoui and A. Khallaayoun, "Internet of Energy (IoE) Adoption for a Secure Semi-Decentralized Renewable Energy Distribution," *Sustainable Energy Technologies and Assessments*, vol. 57, p. 103307, 2023.

[8] H. Touhs, A. Temouden, A. Khallaayoun, M. Chraibi and H. El Hafdaoui, "A Scheduling Algorithm for Appliance Energy Consumption Optimization in a Dynamic Pricing Environment," *World Electric Vehicle Journal*, vol. 15, no. 1, p. 1, 2023.

[9] Q. Chen, Z. Kuang, X. Liu and T. Zhang, "Transforming a solar-rich county to an electricity producer: Solutions to the mismatch between demand and generation," *Journal of Cleaner Production*, vol. 336, p. 130418, 2022.

[10] M. Žnidarec, D. Šljivac, G. Knežević and H. Pandžić, "Double-layer microgrid energy management system for strategic short-term operation scheduling," *International Journal of Electrical Power & Energy Systems*, vol. 157, p. 109816, 2024.

[11] S. Ouédraogo, G. A. Faggianelli, G. Notton, J. L. Duchaud and C. Voyant, "Impact of electricity tariffs and energy management strategies on PV/Battery microgrid performances," *Renewable Energy*, vol. 199, pp. 816-825, 2022.

[12] P. Balakumar, T. Vinopraba and K. Chandrasekaran, "Deep learning based real time Demand Side Management controller for smart building integrated with renewable energy and Energy Storage System," *Journal of Energy Storage*, vol. 58, p. 106412, 2023.

[13] M. Rawa, Y. Al-Turki, K. Sedraoui, S. Dadfar and M. Khaki, "Optimal operation and stochastic scheduling of renewable energy of a microgrid with optimal sizing of battery energy storage considering cost reduction," *Journal of Energy Storage*, vol. 59, p. 106475, 2023.

[14] B. Mukhopadhyay and D. Das, "Optimal multi-objective long-term sizing of distributed energy resources and hourly power scheduling in a grid-tied microgrid," *Sustainable Energy, Grids and Networks*, vol. 30, p. 100632, 2022.

[15] M. M. U. Rashid, M. A. Hossain, R. Shah, M. S. Alam, A. K. Karmaker and M. Rahman, "An Improved Energy and Cost Minimization Scheme for Home Energy Management (HEM) in the Smart Grid Framework," in *IEEE International Conference on Applied Superconductivity and Electromagnetic Devices (ASEMD)*, Tianjin, China, 2020.

[16] X. M. Zhang, K. Grolinger, M. A. M. Capretz and L. Seewald, "Forecasting Residential Energy Consumption: Single Household Perspective," in *17th IEEE International Conference on Machine Learning and Applications (ICMLA)*, Orlando, FL, USA, 2018.

[17] H. El Hafdaoui, A. Khallaayoun, I. Bouarfa and K. Ouazzani, "Machine learning for embodied carbon life cycle assessment of buildings," *Journal of Umm Al-Qura University for Engineering and Architecture*, vol. 14, no. 3, p. 188–200, 2023.

[18] Agence Nationale pour le Développement des Energies Renouvelables et de l'Efficacité Energétique (ADEREE), "Réglement Thermique de Construction au Maroc (RTCM)," United Nations Development Programme (UNDP), Rabat, Morocco, 2021.